



LAWRENCE
LIVERMORE
NATIONAL
LABORATORY

The molecular to atomic phase transition in high pressure hydrogen

J. McMinis, R. C. Clay, M. A. Morales

January 17, 2014

Physical Review Letters

Disclaimer

This document was prepared as an account of work sponsored by an agency of the United States government. Neither the United States government nor Lawrence Livermore National Security, LLC, nor any of their employees makes any warranty, expressed or implied, or assumes any legal liability or responsibility for the accuracy, completeness, or usefulness of any information, apparatus, product, or process disclosed, or represents that its use would not infringe privately owned rights. Reference herein to any specific commercial product, process, or service by trade name, trademark, manufacturer, or otherwise does not necessarily constitute or imply its endorsement, recommendation, or favoring by the United States government or Lawrence Livermore National Security, LLC. The views and opinions of authors expressed herein do not necessarily state or reflect those of the United States government or Lawrence Livermore National Security, LLC, and shall not be used for advertising or product endorsement purposes.

The molecular to atomic phase transition in high pressure hydrogen

Jeremy McMinis and Miguel Morales*

Lawrence Livermore National Laboratory, Livermore, California USA 94550

Raymond Clay III

University of Illinois, Urbana, Illinois USA 61821

(Dated: January 16, 2014)

The metallization of high pressure hydrogen, together with the associated molecular-to-atomic transition, is one of the most important problems in the field of high pressure physics. It is also currently a matter of intense debate due to the existence of conflicting experimental reports on the observation of metallic hydrogen on a diamond anvil cell¹⁻³. Theoretical calculations, mostly based on a mean-field description of electronic correlation through density functional theory, have not been able to provide much light on this problem so far, due to their known limitations in the description of metal-insulator transitions. In fact, as shown recently^{4,5}, the predictions of the pressure driven dissociation of molecules in high pressure hydrogen by density functional theory is strongly affected by the chosen exchange-correlation functional. In this article we use highly accurate quantum Monte Carlo calculations to study the molecular-to-atomic transition in hydrogen. Quantum Monte Carlo has been shown to produce benchmark results for many materials in the periodic table, particularly light elements like hydrogen. We obtain a transition pressure of 439(3) *GPa*, in excellent agreement with the best experimental estimate of the transition, 450 *GPa*, based on an extrapolation to zero band gap from experimental measurements⁶. Also in agreement with experimental measurements, our calculations do not produce additional molecular-to-molecular transitions between the molecular phase III (*C2/c*) and the atomic phase, in contrast to all DFT calculations that predict multiple molecular phases in between.

Hydrogen is the simplest and most abundant atom in the universe, yet its behavior at high pressures is one of the most puzzling^{7,8}. Being the lightest element in the periodic table, its strong quantum nature at low temperatures and subtle electronic structure leads to very interesting physics which include: multiple orientationally-ordered molecular phases^{2,3,9}, a re-entrant melting line¹⁰⁻¹³, a liquid-liquid phase transition¹⁴⁻¹⁶, and a metal-insulator transition accompanied with the possibility of exotic physics including superconductivity¹⁷ and a zero-temperature liquid¹⁸. Describing the physics of these processes and its equation of state with quantitative accuracy is of critical importance to many areas of physics including astrophysics, planetary science, material science, and inertial confinement fusion research.

Since the original prediction by Wigner and Huntington, experimentalists and theorists have tirelessly pursued the creation, observation, and the quantitatively accurate description of metallic hydrogen. Because hydrogen is highly reactive and diffusive, attempts to experimentally synthesize metallic hydrogen in diamond-anvil cell experiments are difficult, and sometimes produce conflicting predictions. It has been claimed that metallic hydrogen may have been observed very recently by Erements, *et al*¹. These findings have yet to be confirmed and are considered highly controversial¹⁹.

To date, the best experimental estimate of the location of the metal-insulator transition is at approximately 450 *GPa*⁶. This estimate was produced by extrapolation of the band gap to zero as a function of pressure and assumes that hydrogen remains in phase III up to the

transition. Because of hydrogen's small x-ray scattering cross-section a definitive determination of whether it remains in this phase through the observed range is difficult. Determining whether it remains in phase III beyond the experimentally accessible regime must be done using *ab initio* methods. We do so by providing an accurate equation of state to confirm the validity of Loubeyre *et al*'s extrapolations.

For a theoretical method to be predictive in this regime both electronic structure (e.g. electronic correlation) and nuclear quantum effects (which are very strong) must be treated accurately⁵. We use diffusion quantum Monte Carlo (DMC) to compute the pressure and enthalpy of the leading candidate structures for hydrogen near the atomic-to-molecular transition and then correct for zero-point energy (ZPE) contributions using DFT within the quasi-harmonic approximation (QHA). As has been shown previously, and reiterated below, DFT by itself does not provide sufficient accuracy to create a qualitatively correct high pressure hydrogen phase diagram. For this reason we choose the more accurate, and expensive, method DMC to compute total energies and also to benchmark three functionals: PBE, vdW-DF, and vdW-DF2²⁰⁻²⁵.

For solids composed of light elements, such as the electron gas²⁶, hydrogen^{15,27} and helium²⁸, DMC provides the most accurate results currently available. Unlike most traditional electronic structure methods, it treats electronic correlation on the same footing as all other energy components, eliminating any potential problems with self-interaction errors or exchange. In addition, it can properly and accurately describe dispersion interac-

tions, leading to an equate description of both atomic and insulating molecular phases, a critical element in the study of metal-insulator transitions. In essence, DMC is the ideal tool to study high pressure hydrogen with predictive accuracy.

While it would be preferable to use DMC for the lattice degrees of freedom as well, it is currently beyond state of the art. Although DFT has been shown to be inaccurate for the electronic structure of these systems, it is typically much better for zero point energies. As shown previously²⁹, in the molecular phase the frequency of the Raman and IR modes depends strongly on choice of exchange correlation functional. To control for this inaccuracy, we screen several exchange correlation functionals using DMC to assess their error describing the molecular potential energy surface. On the atomic side we find that all functionals predict similar zero point energies and that functional choice is inessential.

Our results show that there is a phase transition directly from the molecular $C2/c$ phase to the atomic $Cs-IV$ phase at 439(3) GPa . It is notable that this transition pressure is in good agreement with Loubeyre *et al.*'s extrapolation, and confirms their assumption of constant phase up to metallization. It also suggests a mechanism for metallization, the molecular to atomic transition. We note the failure of DFT to predict the correct phase structure. All functionals predict spurious molecular phases, $Cmca-12$ and $Cmca$, for both the static and dynamic lattice. We begin below with a brief description of our computational procedure in the molecular and atomic phases using both DFT and DMC. In depth discussion of these procedures and method can be found in the supplementary material and references. We then present our results for the transition pressure from molecular to atomic hydrogen. We conclude with a discussion of our findings in light of previous theory and experiment.

Results- To compute the location of the molecular to atomic phase transition we start with a selection of the most important candidate structures for each phase and optimize their geometry. On the atomic side we selected the only 2 competing phases: β -tin and $Cs-IV$. Since both of these structures have only 1 variable parameter in their geometry, namely the c/a ratio, we directly optimized their geometries with DMC at several volumes in the pressure range 450 – 800 GPa . On the molecular side we selected the three candidate phases: $C2/c$, $Cmca$, and $Cmca-12$. The large number of degrees of freedom in these structures prevent us from a direct optimization of the geometry with DMC. Instead, we optimized the geometries and atomic positions at selected pressures using three different DFT exchange correlation functionals (vdW-DF, vdW-DF2, PBE) and performed a detailed comparison of the resulting energies. On the one hand, this will allow us to identify any possible dependence of the structure and its DMC energy on the functional used to optimize it. On the other hand, in case that dependence is strong, it will allow us to choose the best structure at each pressure, getting closer to the

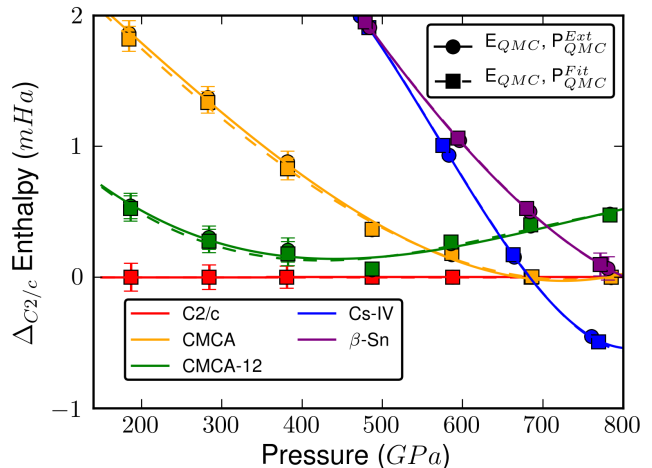


FIG. 1: Static lattice enthalpy of molecular and atomic phases relative to the molecular $C2/c$ crystal. The phase transition happens at 684(3) GPa . Circles refer to enthalpies calculated with pressures obtained directly from QMC, while squares refer to enthalpies calculated with pressures obtained from fits to the energy as a function of volume. Notice how both approaches lead to nearly identical enthalpies.

true optimized geometry. For all structures and pressures considered in this work, the vdW-DF functional provided the best ground state geometries. The difference in enthalpy between structures optimized at similar pressures with different functionals was found to be as large as 0.4 $mHa/atom$, with the structures produced by PBE always consistently worse than those generated by either vdW-DF or vdW-DF2. In all calculations we are careful to control for finite size effects using twist averaging and supercell size extrapolation to the thermodynamic limit. We refer the reader to the work of Clay, *et al.*³⁰, for a detailed analysis of the quality of various density functionals on the molecular phase, benchmarked against DMC.

Figure 1 shows the enthalpy of the lattice with clamped protons (without zero point energy) for all the structures considered in this work between 200 and 800 GPa . The pressure is calculated directly from DMC using a fit to the equation of state (P^{Fit}) and using the extrapolated virial estimator (P^{Ext}). The extrapolated pressure estimator has the form: $P^{Ext} = 2P^{DMC} - P^{VMC}$ where $P = (2K + V)/(3\Omega)$, where K, V , and Ω correspond to the kinetic energy, potential energy and volume and VMC, DMC refer to the level of theory used to compute them. This extrapolation removes the leading source of error due to the trial wave function. Both curves are in excellent agreement and shown in Figure 1. This provides confidence that our calculations have little systematic error. Our QMC calculations show that the molecular-to-atomic transition in the absence of ZPE occurs at 684(3) GPa , directly between the $C2/c$ and the $Cs-IV$ phases.

Our results show both qualitative and quantitative disagreement between QMC and DFT for the electronic

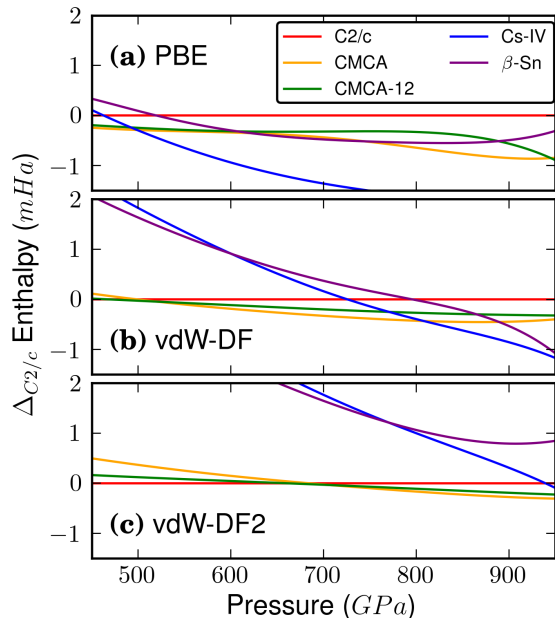


FIG. 2: DFT electronic structure contribution to Enthalpy for three functionals: (a) PBE, (b) vdW-DF and (c) vdW-DF2. Note that in contradiction to the QMC results, all exchange correlation functionals predict a molecular-molecular transition before the molecular to atomic transition. The vdW-DF transition location is in best agreement with QMC.

structure near disassociation. The enthalpy as a function of pressure for the candidate ground state structures for all DFT functionals considered in this work, PBE, vdW-DF and vdW-DF2, are shown in Figure 2. All predict several molecular to molecular phase transitions ($C2/c \rightarrow Cmca-12 \rightarrow Cmca$) before the atomic phase is reached. In addition, the location of the transition is in very poor agreement with the QMC predictions. According to PBE, the transition occurs around 500 GPa between $Cmca$ and $Cs-IV$ structures, which is around 185 GPa too low. Both vdW functionals predict much higher transitions, by almost 100 GPa and 300 GPa for the vdW-DF and vdW-DF2 respectively.

The results for the static lattice show the strong dependence of the molecular disassociation pressure on the functional’s relative accuracy in the metallic and molecular states. However, no prediction can be made without a careful treatment of the ZPE. As mentioned previously, an accurate treatment of the ZPE with DMC is beyond the current capabilities of the method. Instead, we must resort to a more approximate treatment within DFT. To make the task more complicated, the ZPE predicted by DFT is quite dependent on the functional used on the molecular phase. As described in the supplementary material³¹, the variations of the magnitude of the ZPE component with DFT functional on the atomic side is on the order of 0.2 mHa/atom and basically independent of structure. On the molecular side,

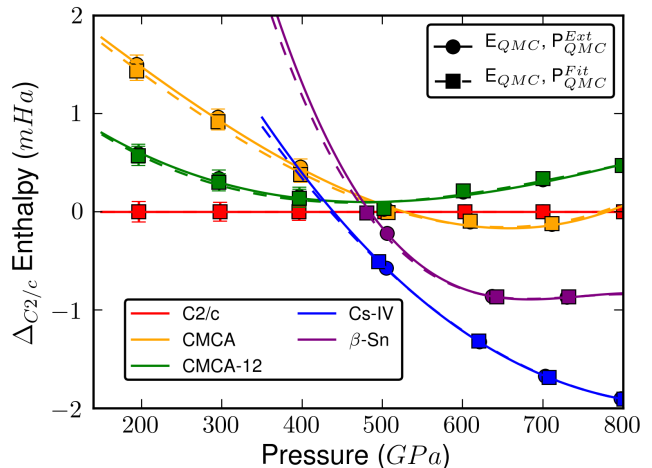


FIG. 3: Enthalpy of molecular and atomic phases relative to the molecular $C2/c$ crystal. We find a phase transition from molecular to atomic hydrogen at 439(3) GPa. Two QMC curves are provided, each using a different estimator to compute the pressure. These two curves provide an estimate on the systematic error of our pressure calculation.

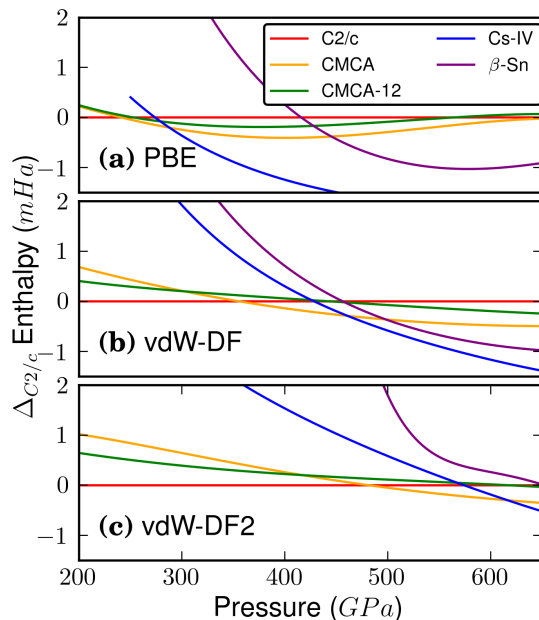


FIG. 4: Enthalpy vs Pressure for three DFT exchange correlation functionals: (a) PBE, (b) vdW-DF and (c) vdW-DF2. Zero point energy shifts the transition down a few hundred GPa for each functional but does not remove the spurious molecular-molecular transition.

the variation is bigger than 1.0 mHa/atom and can be as large as 2 mHa/atom. This large variation in the magnitude of the ZPE will strongly bias any prediction of the molecular-to-atomic transition because the characteristic energy difference in enthalpy for these phases is also of order mHa/atom.

In contrast to the atomic phase, in the molecular phase intramolecular vibrations provide the dominant contribution to the ZPE. As shown in the work of Clay, *et al.*,³⁰ and described in the supplementary material³¹, there is a strong variation in the description of the molecular bond and the corresponding intramolecular potential between the different DFT functionals. This variation leads to the observed discrepancy on the magnitude of the ZPE in each phase. Using correlated sampling combined with reptation quantum Monte Carlo, we calculate the dependence of the energy of the crystal with molecular bond length. This allows us to optimize the bond lengths with DMC, compared them against DFT results, as well as to measure the curvature of the molecular potential at the equilibrium bond length, which is directly related to the vibrational frequency of the molecule and to the magnitude of the ZPE.

We find that the vdW-DF functional produces the best overall agreement in all aspects of the molecular bond in hydrogen: the magnitude of the bond length (accurate to $\approx 1\%$), pressure dependence, and the curvature of the intramolecular potential. Notice that PBE systematically, and significantly, overestimates the magnitude of the bond length (by up to $\approx 5\%$), and in addition it systematically underestimates the curvature of the potential, leading to much lower zero-point energies for all the structures. vdW-DF2, on the other hand, systematically underestimates the bond lengths (by up to $\approx 4\%$) and overestimates the curvature. We conclude that vdW-DF provides the most accurate estimate of the ZPE in these molecular phases, due to its good agreement with QMC, and choose it to provide the ZPE contribution we use for our QMC results. The agreement between vdW-DF and QMC is consistent with the recent benchmark of DFT functionals³⁰, where it is shown that the vdW-DF functional produces the most accurate shape of the potential energy surface for molecular phases.

Our main result, the total enthalpy (including electronic contribution and ZPE) of all the structures considered in this work, is shown in Figure 3. We find a molecular to atomic phase transition at 439(3) *GPa* between the *C2/c* and *Cs-IV* phases. The transition pressure is in excellent agreement with the best experimental estimates of metallization as suggests they occur simultaneously⁶.

As was the case without ZPE, when ZPE is included DFT is both qualitatively and quantitatively inaccurate. Figure 4 shows the enthalpy as a function of pressure obtained with these three DFT functionals. ZPE contributions shift the phase transition downwards between 200 for PBE to 400 *GPa* for vdW-DF2 and reduces the region of stability for the spurious *Cmca* phase. The resulting molecular disassociation transition ranges from 288 for PBE to 617 *GPa* for vdW-DF2 with only the vdW-DF function close to the QMC result at 461 *GPa*.

It is worth noting that according to PBE at low temperatures atomic hydrogen is stable at pressures above 288 *GPa*, which is in complete disagreement with experimental observations. PBE systematically fails to accu-

rately describe hydrogen close to the dissociation regime. On the one hand, it provides a very poor description of the intramolecular interaction by greatly overestimating the bond length and underestimating the curvature of the potential (and hence the vibrational frequency). On the other hand, it strongly reduces the energy of the atomic phases relative to the molecular ones, leading to very low transition pressures. To the authors knowledge, the low dissociation pressure produced by PBE has not been explicitly mentioned in previous published work.

Conclusions- The promise of observing metallic hydrogen at low temperature is within close reach of current experimental techniques. Our calculation places the molecular to atomic transition pressure at 439(3) *GPa*, which is in good agreement with the experimental extrapolation to metallization and not far above the current experimental range. We also predict a direct transition from the *C2/c* structure in the molecular phase to the atomic *Cs-IV* structure. This simplifies the interpretation of experimental results and justifies Loubeyre *et al.*'s extrapolation.

Using a combination of highly accurate DMC calculations and well screened DFT results, this work represents the most accurate study of the molecular to atomic transition in high pressure hydrogen to date. We have illustrated the deficiencies of a DFT only approach to the problem and provided guidance in the selection of functionals in this regime to compliment more accurate yet expensive methods such as QMC. We believe that the QMC plus DFT approach used in this paper will be broadly useful for obtaining quantitatively accurate phase diagrams in high pressure.

Methods All QMC calculations were performed with the Quantum Monte Carlo Package (QMCPACK)³². We used the full Coulomb potential and a Slater-Jastrow trial wave function. The Jastrow consists of one and two body B-spline terms. We optimize all variational parameters using the linear method³³ at a single twist near the Γ -point and subsequently use it for all twists. The single particle orbitals are generated using the quantum espresso density functional theory code³⁴. We use a PBE exchange correlation functional and a norm-conserving pseudopotential generated using OPIUM with a cutoff radius of 0.5 bohr. We converge the wave functions with a 200 Ry cutoff. We used twist-averaged boundary conditions³⁵ in all DMC calculations, with a 24^3 K-point grid for the 4 atom unit cell in the atomic phase and 6^3 K-point grid for the 96 atom unit cell in the molecular phase. Simulation cells of various sizes were used to extrapolate the energies to the thermodynamic limit³¹. Pressures were computed using the extrapolated virial estimator, as well as by differentiation of the energy.

DFT calculations were performed with the Vienna Ab-Initio Simulation Package (*VASP*)^{36,37}. We used the projector augmented wave (PAW) representation of *VASP*, with a PAW constructed with PBE from their most recent release. A plane-wave cutoff of 1000 eV was used in all geometry optimizations, final enthalpies were cal-

culated with a cutoff of 1400 eV. Different k-point grids were used in the DFT calculations, since the number of atoms in the primitive unit cells vary from 4 to 48. We carefully checked that results were well converged in both optimizations and final enthalpy calculations. All ZPE calculations reported on this article were calculated with the *Phonopy* code (<http://phonopy.sourceforge.net/>) and were based on the quasi-harmonic approximation. All ZPE calculations on the molecular phases employed 728 atoms, while all calculations on the atomic phase employed 432 atoms. We carefully tested that the resulting ZPEs were well converged by using cells with up to 2592 and 1600 atoms on the molecular and atomic phase re-

spectively. Convergence with k-points and plane-wave cutoff were also carefully tested.

Acknowledgments- J. B. M. and M. A. M. acknowledge useful conversations with Jeffrey M. McMahon, David M. Ceperley, Ethan Brown, Jonathan Dubois, Sebastian Hamel, Randy Hood, Stanimir Bonev and Sarang Gopalakrishnan. M. A. M. and J. B. M. were supported by the U.S. Department of Energy at the Lawrence Livermore National Laboratory under Contract DE-AC52-07NA27344 and by LDRD Grant No. 13-LW-004. Computer resources have been provided by Lawrence Livermore National Laboratory through the 7th Institutional Unclassified Computing Grand Challenge program.

* Electronic address: moralessilva2@llnl.gov

- ¹ Eremets, M. & Troyan, I. Conductive dense hydrogen. *Nature materials* **10**, 927–931 (2011).
- ² Howie, R. T., Guillaume, C. L., Scheler, T., Goncharov, A. F. & Gregoryanz, E. Mixed molecular and atomic phase of dense hydrogen. *Physical Review Letters* **108**, 125501 (2012).
- ³ Zha, C.-s., Liu, Z., Ahart, M., Boehler, R. & Hemley, R. J. High-pressure measurements of hydrogen phase iv using synchrotron infrared spectroscopy. *Phys. Rev. Lett.* **110**, 217402 (2013).
- ⁴ Morales, M. A., McMahon, J. M., Pierleoni, C. & Ceperley, D. M. Nuclear Quantum Effects and Nonlocal Exchange-Correlation Functionals Applied to Liquid Hydrogen at High Pressure. *Physical Review Letters* **110**, 065702 (2013). URL <http://link.aps.org/doi/10.1103/PhysRevLett.110.065702>.
- ⁵ Morales, M. A., McMahon, J. M., Pierleoni, C. & Ceperley, D. M. Towards a predictive first-principles description of solid molecular hydrogen with density functional theory. *Physical Review B* **87**, 184107 (2013).
- ⁶ Loubeyre, P., Occelli, F. & LeToullec, R. Optical studies of solid hydrogen to 320 GPa and evidence for black hydrogen. *Nature* **416**, 613–7 (2002). URL <http://www.ncbi.nlm.nih.gov/pubmed/11948345>.
- ⁷ Chang, K. The big squeeze. *The New York Times* (2013). URL <http://www.nytimes.com/2013/12/17/science/the-big-squeeze.html?pagewanted=all&r=0>.
- ⁸ McMahon, J. M., Morales, M. A., Pierleoni, C. & Ceperley, D. M. The properties of hydrogen and helium under extreme conditions. *Reviews of Modern Physics* **84**, 1607 (2012).
- ⁹ Mao, H.-k. & Hemley, R. J. Ultrahigh-pressure transitions in solid hydrogen. *Rev. Mod. Phys.* **66**, 671–692 (1994).
- ¹⁰ Bonev, S. A., Schwegler, E., Ogitsu, T. & Galli, G. A quantum fluid of metallic hydrogen suggested by first-principles calculations. *Nature* **431**, 669–72 (2004). URL <http://www.ncbi.nlm.nih.gov/pubmed/15470423>.
- ¹¹ Deemyad, S. & Silvera, I. Melting Line of Hydrogen at High Pressures. *Physical Review Letters* **100**, 155701 (2008). URL <http://link.aps.org/doi/10.1103/PhysRevLett.100.155701>.
- ¹² Eremets, M. I. & Trojan, I. A. Evidence of maximum in the melting curve of hydrogen at megabar pressures. *JETP Letters* **89**, 174–179 (2009). URL <http://link.springer.com/10.1134/S0021364009040031>.
- ¹³ Subramanian, N., Goncharov, A. F., Struzhkin, V. V., Somayazulu, M. & Hemley, R. J. Bonding changes in hot fluid hydrogen at megabar pressures. *Proceedings of the National Academy of Sciences of the United States of America* **108**, 6014–9 (2011). URL <http://www.pubmedcentral.nih.gov/articlerender.fcgi?artid=3076824&tool=pmcentrez&rendertype=abstracthttp://www.pnas.org/content/108/15/6014.short>.
- ¹⁴ Scandolo, S. Liquid-liquid phase transition in compressed hydrogen from first-principles simulations. *Proceedings of the National Academy of Sciences of the United States of America* **100**, 3051–3 (2003). URL <http://www.pubmedcentral.nih.gov/articlerender.fcgi?artid=152244&tool=pmcentrez&rendertype=abstract>.
- ¹⁵ Morales, M. A., Pierleoni, C., Schwegler, E. & Ceperley, D. M. Evidence for a first-order liquid-liquid transition in high-pressure hydrogen from ab initio simulations. *Proceedings of the National Academy of Sciences of the United States of America* **107**, 12799–803 (2010). URL <http://www.pubmedcentral.nih.gov/articlerender.fcgi?artid=2919906&tool=pmcentrez&rendertype=abstract>.
- ¹⁶ Dzyabura, V., Zaghoo, M. & Silvera, I. F. Evidence of a liquidliquid phase transition in hot dense hydrogen. *Proceedings of the National Academy of Sciences* **110**, 8040–8044 (2013). URL <http://www.pnas.org/content/110/20/8040.abstract>. <http://www.pnas.org/content/110/20/8040.full.pdf+html>.
- ¹⁷ Babaev, E., Sudbø, A. & Ashcroft, N. W. A superconductor to superfluid phase transition in liquid metallic hydrogen. *Nature* **431**, 666–8 (2004). URL <http://www.ncbi.nlm.nih.gov/pubmed/15470422>.
- ¹⁸ Chen, J. *et al.* Quantum simulation of low-temperature metallic liquid hydrogen. *Nat Commun* **4** (2013).
- ¹⁹ Nellis, W. J., Ruoff, A. L. & Silvera, I. F. Has Metallic Hydrogen Been Made in a Diamond Anvil Cell? *arXiv preprint arXiv:1201.0407* **8** (2012). URL <http://arxiv.org/abs/1201.0407>. 1201.0407.
- ²⁰ Perdew, J. P., Burke, K. & Ernzerhof, M. Generalized gradient approximation made simple. *Physical review letters* **77**, 3865 (1996).
- ²¹ Dion, M., Rydberg, H., Schröder, E., Langreth, D. C. & Lundqvist, B. I. Van der waals density functional for general geometries. *Physical review letters* **92**, 246401 (2004).

- ²² Thonhauser, T. *et al.* Van der waals density functional: Self-consistent potential and the nature of the van der waals bond. *Physical Review B* **76**, 125112 (2007).
- ²³ Román-Pérez, G. & Soler, J. M. Efficient implementation of a van der waals density functional: application to double-wall carbon nanotubes. *Physical review letters* **103**, 096102 (2009).
- ²⁴ Lee, K., Murray, É. D., Kong, L., Lundqvist, B. I. & Langreth, D. C. Higher-accuracy van der waals density functional. *Physical Review B* **82**, 081101 (2010).
- ²⁵ Klimeš, J., Bowler, D. R. & Michaelides, A. Chemical accuracy for the van der waals density functional. *Journal of Physics: Condensed Matter* **22**, 022201 (2010).
- ²⁶ Ceperley, D. M. & Alder, B. J. Ground State of the Electron Gas by a Stochastic Method. *Physical Review Letters* **45**, 566–569 (1980). URL <http://link.aps.org/doi/10.1103/PhysRevLett.45.566><http://link.aps.org/doi/10.1103/PhysRevLett.56.2415>.
- ²⁷ Morales, M. A., Pierleoni, C. & Ceperley, D. M. Equation of state of metallic hydrogen from coupled electron-ion Monte Carlo simulations. *Physical Review E* **81**, 1–9 (2010). URL <http://link.aps.org/doi/10.1103/PhysRevE.81.021202>.
- ²⁸ Khairallah, S. A. & Militzer, B. First-principles studies of the metallization and the equation of state of solid helium. *Phys. Rev. Lett.* **101**, 106407 (2008). URL <http://link.aps.org/doi/10.1103/PhysRevLett.101.106407>.
- ²⁹ Azadi, S. & Foulkes, W. M. C. Fate of density functional theory in the study of high-pressure solid hydrogen. *Phys. Rev. B* **88**, 014115 (2013).
- ³⁰ Clay, R. C. *et al.* Benchmark of exchange-correlation functionals for high pressure hydrogen using quantum monte carlo. *submitted to Phys. Rev. B* (2013).
- ³¹ Supplementary material.
- ³² Kim, J. *et al.* Hybrid algorithms in quantum monte carlo. *Journal of Physics: Conference Series* **402**, 012008 (2012). URL <http://stacks.iop.org/1742-6596/402/i=1/a=012008>.
- ³³ Umrigar, C. J., Toulouse, J., Filippi, C., Sorella, S. & Hennig, R. G. Alleviation of the Fermion-Sign Problem by Optimization of Many-Body Wave Functions. *Physical Review Letters* **98**, 110201 (2007). URL <http://link.aps.org/doi/10.1103/PhysRevLett.98.110201>.
- ³⁴ Giannozzi, P. *et al.* QUANTUM ESPRESSO: a modular and open-source software project for quantum simulations of materials. *Journal of physics. Condensed matter : an Institute of Physics journal* **21**, 395502 (2009). URL <http://www.ncbi.nlm.nih.gov/pubmed/21832390>.
- ³⁵ Lin, C., Zong, F. & Ceperley, D. Twist-averaged boundary conditions in continuum quantum monte carlo algorithms. *Physical Review E* **64**, 016702 (2001).
- ³⁶ Kresse, G. & Furthmüller, J. Efficiency of ab-initio total energy calculations for metals and semiconductors using a plane-wave basis set. *Computational Materials Science* **6**, 15–50 (1996). URL <http://linkinghub.elsevier.com/retrieve/pii/0927025696000080>.
- ³⁷ Kresse, G. & Joubert, D. From ultrasoft pseudopotentials to the projector augmented-wave method. *Physical Review B* **59**, 1758–1775 (1999). URL <http://link.aps.org/doi/10.1103/PhysRevB.59.1758>.

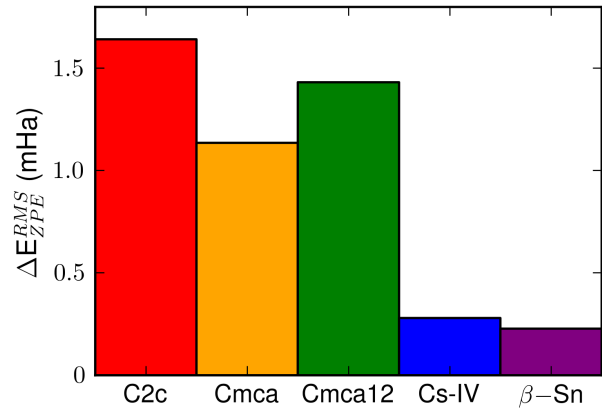


FIG. 5: Root mean squared difference for the largest and smallest zero point energy for different symmetry structures. The difference in ZPE between functionals is much greater in the molecular phases.

I. SUPPLEMENTARY INFORMATION

A. Zero Point Energy Contributions

When the lattice is allowed to move additional terms contribute to the energy, enthalpy, and pressure. These zero point energy (ZPE) effects are important to include for the prediction of accurate transition pressures. This is particularly important for the dissociation transition, where the magnitude of the ZPE is considerably different between atomic and molecular phases. Because DMC calculations with dynamic protons are prohibitively expensive, we include these lattice effects using density functional theory in the harmonic approximation.

We compute the zero point energy of each lattice using the van der Waals density functional vdW-DF at the minimum energy configuration for each pressure. For the molecular phases this corresponds to the same configurations used in the DMC calculations. In the atomic phase, the minimums are located at a different C/A from the DMC ones. We compute the zero point energy as a function of volume for the *Cs-IV* and *β-tin* phases to add to our DMC results. The ZPE is fit to a cubic polynomial and differentiated to compute the pressure contribution. The contribution to the enthalpy is the sum of these two terms,

$$\Delta H = E_{ZPE} + \Omega P_{ZPE} \quad (1)$$

$$P_{ZPE} = -\frac{\partial E_{ZPE}}{\partial \Omega} \quad (2)$$

where H is the enthalpy, E_{ZPE} is the zero point energy, Ω is the volume, and P_{ZPE} is the pressure contribution from the changing zero point energy.

Figure 5 illustrates the difference in the magnitude of the ZPE predicted by the functionals considered in this work. While the variations in the atomic side are small, the variations in the molecular side are large enough to

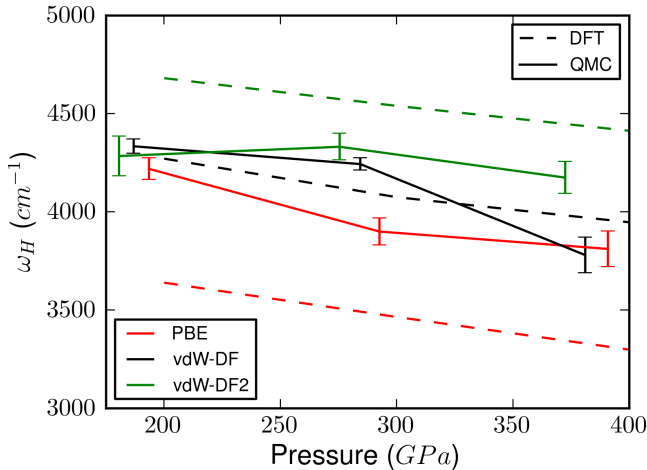


FIG. 6: Harmonic Frequency, ω , for the hydrogen molecule in the $C2/c$ phase. Dashed lines are DFT, solid lines are QMC. Colors encode the exchange correlation functional used to relax the structure and for computing the DFT frequencies. The QMC frequencies are in better agreement with each other, and agree best with the vdW-DF functional. Raw data from reference³⁰.

significantly modify predictions in the phase diagram. Because of this sensitivity to the calculated ZPE, we are careful to choose the best one when computing the transition pressures for the dynamic lattice. As shown in a

recent publication from the authors³⁰, the vdW-DF density function predicts the most accurate energy differences for perturbations to the perfect lattice for all the phases considered here.

In the molecular phase, it has been noted that the vibrational density of states (VDOS) at low frequency is largely independent of choice of functional. It is the high energy, intramolecular modes which make the largest contribution to the differences between the zero point energy of the phase as found by each functional. To screen the accuracy of the intramolecular potential energy surface, we compute the energy of the molecular solids as a function of the hydrogen bond length. We use this to compute a vibrational frequency of the molecule which is closely related to the Raman modes observed in experiment. In Figure 6 we illustrate the frequency obtained using correlated sampling DMC, and DFT across a range of pressures. The structures used for each functional is relaxed using the same functional for consistency. Because of differences in these structures it is not expected for them to lie exactly on the same line.

Using the difference between the DMC and DFT frequency, we can estimate a qualitative correction to the VDOS. We use the difference between them, $\Delta\omega = \omega_{DMC} - \omega_{DFT}$ to shift the location of the molecular peak in the VDOS. As shown in Figure 7, this shift brings the VDOS for differing functionals into much better agreement with each other, and clusters them around the vdW-DF functional.

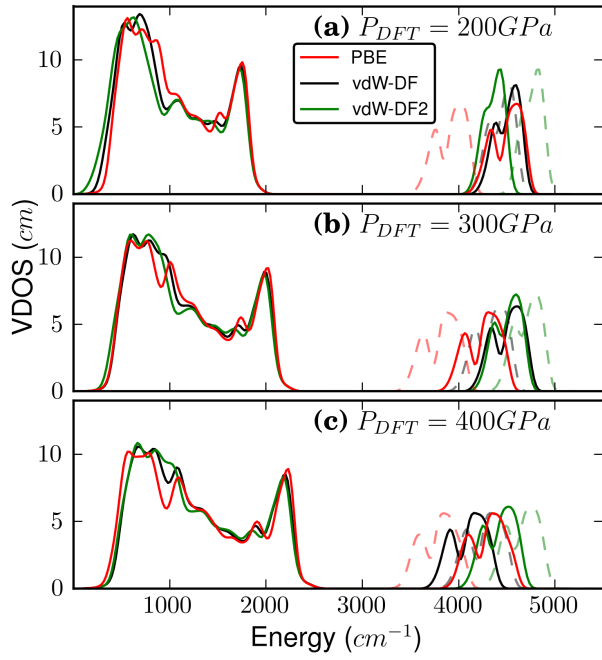


FIG. 7: Vibrational density of states (VDOS) for the $C2/c$ phase at DFT pressures of a) 200 GPa, 300 GPa, and 400 GPa. Colors encode the exchange correlational functional used to relax the structure and used in the DFT claculations. The dashed lines are the uncorrected DFT results. The solid results are the DFT results with QMC corrections which are obtained from Figure 6 and described in the text. After correction, the spread in the high energy components are smaller and more closely bracket the vdW-DF results.